

## **Application of CFD to the design of the runner of a propeller turbine for small hydroelectric power plants**

## **Aplicación de CFD para el diseño del rodete de una turbina tipo hélice para pequeñas centrales hidroeléctricas**

*Edwin Lenin Chica Arrieta\**, Sergio Agudelo Flórez, Natalia Isabel Sierra

Department of Mechanical Engineering. Faculty of Engineering. University of Antioquia. Calle 67 No. 53-108. Medellín, Colombia.

(Recibido el 21 de noviembre de 2012. Aceptado 11 de octubre de 2013)

### **Abstract**

A procedure for the design of the runner of a pico hydraulic propeller turbine according to the specific conditions of water potential of the site of operation is presented based on a theoretical and technical analysis. For this purpose the main characteristics of the runner are determined and data such as the suction head, the rated flow, and the occurring forces are established during the design. Modern engineering tools such as Computational Fluid Dynamics (CFD) are utilized for predicting the flow and Computer Aided Engineering software (CAE) for the design verification.

The Runner of the Propeller Turbines (RPT) designed can be a viable option for electricity generation in not interconnected zones (NIZ) of the national interconnected electric system in developing countries and can be manufacture locally.

**Keywords:** Propeller turbine, small hydropower, rural electrification, CFD, CAE, NIZ

### **Resumen**

En este artículo se presenta un procedimiento para el diseño del rodete de una turbina hidráulica tipo hélice de acuerdo con las condiciones específicas del potencial del agua del sitio de operación basado en un análisis teórico y técnico. Para este fin, las principales características del rodete se determinan y datos tales como la cabeza de succión, el caudal nominal, y las fuerzas que

---

\* Autor de correspondencia: teléfono: +57 4 2198553, correo electrónico: echica@udea.edu.co (E. Chica)

se producen son establecidos durante el diseño. Para la verificación del diseño se utilizan herramientas modernas de ingeniería tales como la dinámica de fluidos computacional (CFD) para predecir el flujo y el método de elementos finitos (CAE) para el chequeo de la integridad estructural.

El rodete diseñado puede ser una opción viable para la generación de energía eléctrica en zonas no interconectadas (ZNI) del sistema interconectado nacional de electricidad en los países en desarrollo y se puede fabricar localmente.

**Palabras clave:** Turbina tipo hélice, pequeñas centrales hidroeléctricas, electrificación rural, CFD, CAE, ZNI

## Introduction

Electrification in some remote areas of developing countries is difficult due to low population densities, highly dispersed location of populated areas, reduced number of service hours (8 hours on average) defaults in payments and customers with low income. In Colombia, approximately 4% of the population that occupy 66% of the national territory is not connected to electricity services through the national interconnected electric system (NIES). These areas are called not interconnected zones (NIZ).

The NIZ in Colombia are characterized by social and economic marginality, deficient or null infrastructure and, in some cases, a difficult situation due to the armed conflict. Today, the electrical installed capacity of these zones is low and is produced using conventional autonomous generation (mainly diesel plants), small hydroelectrics or photovoltaic plants. The main difficulties in the electricity generation in these areas are the access and cost of the fuel [1].

In Colombia, there are many sites where people have a source of water but do not have electricity. Increase the installed capacity in these areas is important to reduce the considerable differences in living conditions existing between in these areas and urban areas of the country. This increase may be possible using the enormous potential of renewable energy sources available in the rural areas.

A recent report on electrification technologies by the World Bank Energy Unit shows that, the hydroelectric in small-scale (pico) can be a cost-

effective option to supply electricity to remote and off-grid areas. The cost of the necessary pico hydro equipment per unit of energy is lower than that of diesel generators, wind turbines or photovoltaic systems, especially when the equipment is locally manufactured [2–6].

Depending on the head and discharge of the sites, the hydroelectric power plant has to be equipped with a specific turbine in order to get the highest efficiency. This paper describes a procedure for the design of the runner of a pico propeller turbine according to the local situation (head  $H$  and flow  $Q$ ) of the NIZ, for pico-hydropower application (systems below 5kW) using modern engineering tools, such as Computational Fluid Dynamics (CFD) and Computer Aided Engineering software (CAE) for the design verification. During the design, the shape of the runner can be optimized according to the flow properties. The runner designed can be manufactured locally.

## Materials and Methods

The RPT is the most important part of a reaction turbine in the power generation. The runner, which is responsible of the conversion of hydraulic energy into mechanical energy, is the most vulnerable component since it is exposed to the load due to the water pressure. The runner has three to six blades of airfoil shape; the number of blades depends of the specific speed. The runner blades are fixed and cannot change their position. The blades are cast integrally with the hub or welded to it. The flow enters the runner through guide vanes which have an angle fixed

and the runner is fully immersed in water, and must be strong enough to withstand the operating pressure [6-12].

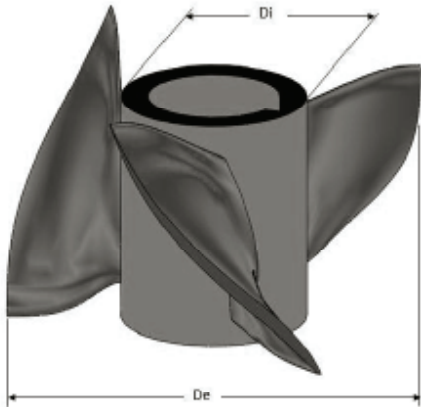
The blade has a very complex geometry that depends of the rated flow (Q) and net head (H) of the site in which the hydroelectric power plant is going to operate. The blades are complex to manufacture due to their irregular shape, and the design is based on airfoil profiles, due to the blades ability to generate a big lift force and a relatively low drag force [11-13].

Based on statistical studies of Kaplan turbines schemes, correlations are established between the geometry of the runner (the runner exterior diameter  $D_e$ , or runner diameter, the runner interior diameter  $D_i$  or hub diameter), the mechanical power produced (P), the rotational speed (N), the

specific speed ( $N_s$ ), the net head (H) and the rated flow (Q). Table 1 presents the aforementioned correlations (equation 1-6), which can be found in the literature. With these correlations it is possible to determinate the external and internal diameter of the runner, however the internal diameter ranges between 30% and 50% of the external diameter [12, 14].

The design of the blade not only depends on the stress analysis, but also in other several factors play a significant role. The leading edge is thicker than the trailing edge for a streamlined flow. Furthermore, the blade should be as thin as possible to reduce cavitation effects. The blade is thicker near the runner interior diameter becoming thinner towards the tip. The wing theory is also an important factor in defining the shape of the profile and the distortion of the blade.

**Table 1** Fundamental dimensions of the runner of propeller turbine

 <p style="text-align: center;"><b>Runner of propeller turbine</b></p>	$P = \eta \rho g Q H \quad (1)$
	$N_s = \frac{N \sqrt{P}}{H^{5/4}} \quad (2)$
	$k_u = 0.79 + 1.61e - 3N_r \quad (3)$
	$D_e = \frac{84.6 k_u \sqrt{H}}{N_r} \quad (4)$
	$D_i = \left( 0.25 + \frac{94.64}{N_r} \right) D_r \quad (5)$ $0.3D_r \leq D_i \leq 0.5D_e$
	$C_m = \frac{4Q}{(D_e^2 - D_i^2)\pi} \quad (6)$

Where P-Mechanical power produced (watts), N-Rotational speed (rev/min),  $N_s$ -Specific speed, Q-Flow rate passing through the turbine ( $m^3/s$ ), H-Effective pressure head of water (m),  $D_e$ -Runner exterior diameter (m),  $D_i$ -Runner interior diameter or hub diameter (m),  $\eta$ -Hydraulic efficiency,  $\rho$ -Water density ( $kg/m^3$ ), g-Acceleration of gravity ( $m/s^2$ ),  $C_m$  Axial velocity (m/s) .

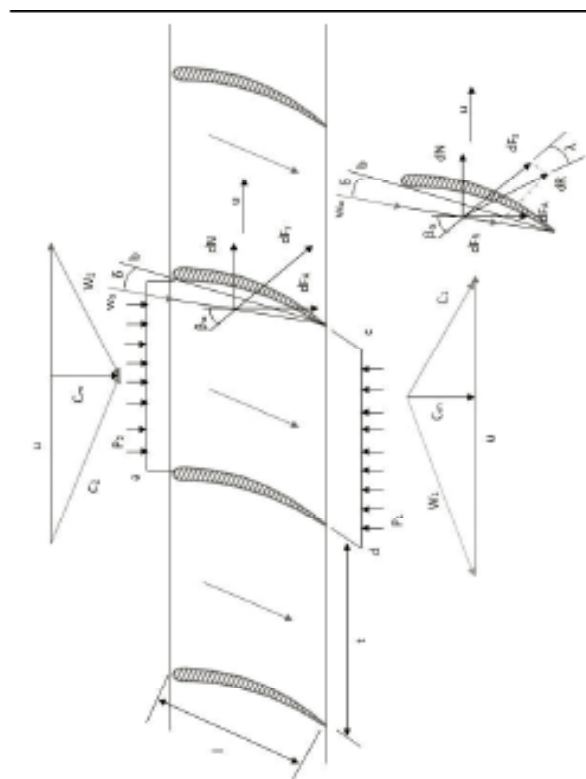

The velocity triangles, which occur on the blade, play a significant role in determining its distortion. The velocities at the velocity triangle

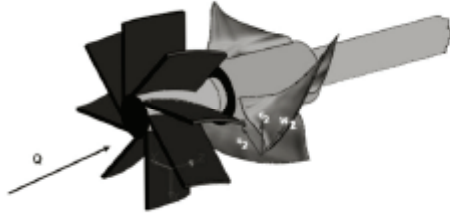
are shown in table 2, where “u” is the tangential velocity, “c” is the absolute velocity and w is the relative velocity. When a cylindrical cut is set at

the runner and the cut is developed into a drawing pane, a grating like that shown in table 2 occurs. In this figure, “t” represents the grating partition and “l” denotes the chord. An approximate solution of the problem of the behavior of the flow through the blades can be obtained considering a constant plane of motion through the grating.

The table also shows the equations used for the hydraulic design of the runner (equation 7-32). These equations can be obtained with theoretical and empirical methods of analysis of flows. The calculation of the blade system was for blades with a degree of reaction between 0.5 and 1.

**Table 2** The velocity triangles, which occur on the blade

	$u = \frac{\pi DN}{60} \quad (7)$
	$Fs = \zeta_a \frac{\gamma W_a^2}{2g} Lb \quad (8)$
	$Fr = \zeta_w \frac{W_w^2}{2g} Lb \quad (9)$
	$\zeta_w = \zeta_w' - \frac{1}{u} \zeta_a^2 \frac{L}{b} \quad (10)$
	$\delta = \delta' - \frac{1}{u} \zeta_a \frac{L}{b} 57.3 \quad (11)$
	$\delta = \frac{\zeta_a - \left(4.8 \frac{Y_{max}}{l}\right)}{0.092} \quad (12)$
<p><b>Velocity vectors on runner blade profile</b></p>	$\epsilon = \tan \lambda = \frac{\zeta_w}{\zeta_a} \quad (13)$
	$\epsilon = 0.12 + 0.0016 \frac{Y_{max}}{l} \quad (14)$
	$\tau = \frac{2r\alpha}{Z} \quad (15)$
<p><b>Velocity triangles</b></p>	$H_x = u\delta c_u \quad (16)$
	$H_R = \eta_h H \quad (17)$
	$H_R = \frac{\zeta_a u}{2g c_m} \frac{W_w^2 L \sin(\beta_a - \lambda)}{\tau \cos \lambda} \quad (18)$
	$c_{2u} = \frac{\beta H_R}{u} \quad (19)$
	$w_a^2 = c_m^2 + \left(u - \frac{c_{2u}}{2}\right)^2 \quad (20)$



Velocity vectors on runner

$$d\dot{m} = \frac{\gamma}{g} t dr c_{\alpha} \quad (19)$$

$$dN = -\frac{\gamma}{g} t dr c_m (w_{2x} - w_{1x}) \quad (20)$$

$$P_2 - P_1 = -\frac{\gamma}{2g} (w_2^2 - w_1^2) \quad (21)$$

$$dF_A = (P_2 - P_1) t dr \quad (22)$$

$$dF_A = -\frac{\gamma}{2g} (w_2^2 - w_1^2) t dr$$

$$\frac{dF_A}{dN} = \frac{(w_2^2 - w_1^2)}{2C_m(w_{2x} - w_{1x})} \quad (23)$$

$$w_2^2 - w_1^2 = w_{2x}^2 - w_{1x}^2 \quad (24)$$

$$\frac{dF_A}{dN} = \frac{(w_{2x}^2 - w_{1x}^2)}{2C_m} = \epsilon t g \beta_{\alpha} \quad (25)$$

$$dR = \frac{dF_s}{\cos \lambda} = \frac{\zeta_{\alpha} \gamma w_{\alpha}^2 dr l}{2g \cos \lambda} \quad (26)$$

$$dN = dR \cos(90 - (\beta_{\alpha} + \lambda)) \quad (27)$$

$$dN = \zeta_{\alpha} \frac{\gamma w_{\alpha}^2}{2g} L dr \frac{\sin(\beta_{\alpha} - \lambda)}{\cos \lambda}$$

$C_{1x} = 0$ , Because the liquid leaving the runner has an axial direction. (28)

$$\zeta_{\alpha} \frac{L}{t} = \frac{2g H_R C_m}{u w_{\alpha}^2 \sin(\beta_{\alpha} - \lambda)} \quad (29)$$

$$dP = \gamma dQ H_R = \gamma Z r n dr C_m H_R = u Z dN \quad (30)$$

$$\tan \beta_{\alpha} = \frac{c_{\alpha}}{u - \frac{C_{2x}}{2}} \quad (31)$$

$$R = \frac{w_{\alpha}}{u} \quad (32)$$

Where,  $u$ -Tangential velocity (m/s),  $c$ -Absolute velocity (m/s),  $w$ -Relative velocity,  $\zeta_w$ -Drag coefficient,  $\zeta_a$ -Lift coefficient,  $r$ -Radius,  $dF_A$ -Axial force,  $l$ -Length of the blade profile or chord,  $Z$ -Number of blades,  $b$ -Profile width,  $F_s$ -Bearing force,  $F_R$ -Resistance Force,  $t$ -step (m),  $W_{\alpha}$ -Relative velocity of blade(m/s),  $\gamma$ -Specific gravity of the fluid,  $\epsilon$ -Glide ratio,  $\lambda$ -Angle of slip. Fuchslocher recommends that the glide ratio is very small so that it can be estimated from 1 to 2 degrees.  $C_1$  and  $C_2$  Absolute velocity (m/s),  $Y_{\max}$ -Represent the maximum ordinates of the top and bottom of the profile (m),  $D$ -Diameter,  $N$ -Rotational speed (rev/min),  $R$ -Degree of reaction,  $W_1$  and  $W_2$  Relative velocity (m/s),  $d\dot{m}$ -Mass flow flowing through the area enclosed by abcd and thickness  $dr$  (kg/s),  $H_R$ -Head of runner,  $P_2$  and  $P_1$  Input and output pressures, respectively,  $dN$  Force exerted by the liquid to blades. (N).

To define the distortion of the blade, the velocity triangles of five different cylindrical sections of the blade, located at a proportional distance, are determined (figure 1). The angle  $\beta^a$  of each radius gives conclusion to the distortion of the

blade, therefore, between the external and internal diameters an arithmetical ratio can be established obtain the diameters

$D_i, D_{i+1}, D_{i+2}, D_{i+3}$  and  $D_e$  or the radii  $r_i, r_{i+1}, r_{i+2}, r_{i+3}$  and  $r_e$  respectively.

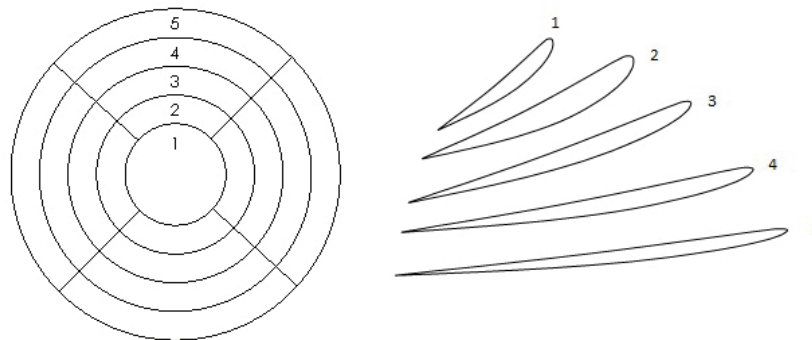


**Figure 1** Cylindrical cuts of the blade

From the design of the profile a type Gottingen N-428 was chosen. The selection was made following recommendation from several authors such as Adolph [15] and Pfeleiderer [16], for applications in turbines and axial pumps. The characteristics of the blade were obtained from

the Institute of Aerodynamics of Göttingen, Germany. Table 3 shows the characteristics of the profile at different sections, expressed as a percentage of the length  $L$ .  $y_0$  and  $y_u$  represent the ordinates of the top and bottom of the profile corresponding to the abscissa  $x$ .

**Table 3** Values in % of the length for the profile Gottingen N-428 [16]

	$x$	0	1.25	2.5	5.0	7.5	10	15	20	30
	$y_0$	1.25	2.75	3.50	4.80	6.05	6.50	7.55	8.20	8.55
<b>Profile</b>	$y_u$	1.25	0.30	0.20	0.10	0.00	0.00	0.05	0.15	0.30
<b>428</b>	$x$	40	50	60	70	80	90	95	100	
	$y_0$	8.35	7.80	6.80	5.50	4.20	2.15	1.20	0.00	
	$y_u$	<b>0.40</b>	<b>0.40</b>	<b>0.35</b>	<b>0.25</b>	<b>0.15</b>	<b>0.05</b>	<b>0.00</b>	<b>0.00</b>	

$y_0$  and  $y_u$  represent the ordinates of the top and bottom of the profile corresponding to the abscissa  $x$ .

The correlations between table 1, table 2 and the profile characteristic of the blade enable a preliminary design of the RPT. For the design it is recommended to use an axial velocity  $C_m < 7$  m/s and a ratio  $t/l$  between 1 and 2, in order to select the best combination of the external diameter and

internal diameters for the runner (from 30% to 50% $D_j$ ) [15, 16]. It should be noted that there are multiple possible combinations between the external and internal diameters from the possible combinations, choose those in which the runner has better symmetry and proportionality of its

blades. Having the values of  $(t/l) > 1$  ensures that the blades are properly spaced. Otherwise, there will be major changes in the fluid path. For values of  $(t/l) > 2$  blades are too spaced out and cannot achieve a good energy transfer. The procedure described for the design of the runner is difficult, time consuming and not always successful. Therefore, another simple procedure is used. The procedure consists in selecting a pair of internal and external diameters that comply with recommendations of the axial velocity and the ratio  $t/l$ . After obtaining the dimensions of the runner and with the assistance of a CAD software, such as Solid Works, the runner is modeled. In order to build the model, it is necessary know the coordinates of the profiles at five or more different cylindrical sections of the blade, located at proportional distances. The coordinates are generated through a series of calculations performed in MSExcel or similar programs. During the design, several profiles are required to increase the control sensitivity on each blade, due to its variable thickness and thirdly, obtaining the correct angle of attack on each section.

Later, CFD can be used in the verification of the hydraulic design of the runner, to give a graphic description of the water flow inside of the propeller turbine and to obtain the velocity and pressures distributions. The boundary conditions should be consistent with the design. This is useful information in the design of the turbine because it helps reduce construction mistakes, or it allows to the geometry of the runner to obtain the design power. In the CFD software is possible to estimate important design parameters such as hydraulic power and torque on the blades of the runner.

The structural integrity of runner can be checked with Computer Aided Engineering software (CAE). During this step, the thickness of the blades can be changed to generate sufficient strength to prevent failure under loading.

In conclusion, the development of the RPT in this paper has followed five steps: planning, design, evaluation (CFD, CAE), and prototyping. Figure 2 shows the general procedure for the design of the runner.

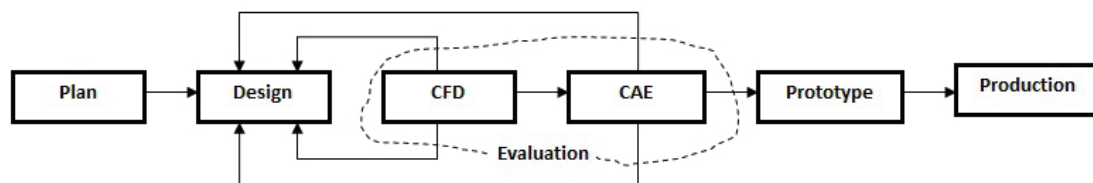


**Figure 2** General procedure for the design of the runner

## Results

The RPT was designed for a head of 4.5 m and a flow of 0.2698 m<sup>3</sup>/s. A moderate working hydraulic efficiency of 60% was assumed and a fixed operating speed of 900 rpm. It was expected that the power generated was equal to 5 kw. The specify speed, the runner diameter, the hub diameter and the characteristics of the blades

profile for different sections can be calculated with some relations of tables 1 and 2. The ratio of the hub diameter to the runner diameter ( $D_h/D_r$ ) is taken to be 0.35. The runner was designed with 3 blades and the guide vanes were designed using correlations found in the technical literature [12]. Table 4 shows the main geometric characteristics of blades.



**Table 4** Main geometric characteristics of blades

<b>Parameter</b>	<b>Values</b>					
	Di	Di+1	Di+2	Di+3	De	Equation
<i>Diameter (m)</i>	0.084	0.123	0.162	0.201	0.240	(4,5)
<i>Radius (m)</i>	$r_i$	$r_{i+1}$	$r_{i+2}$	$r_{i+3}$	$r_e$	-
	0.042	0.0615	0.081	0.100	0.120	-
<i>u(m/s)</i>	3.958	5.796	7.634	9.472	11.309	(7)
<i>C<sub>2u</sub> (m/s)</i>	7.137	4.874	3.701	2.983	2.498	(16)
<i>W<sub>α</sub><sup>2</sup> (m/s)</i>	44.046	55.178	77.345	107.58	145.112	(18)
<i>tan β<sub>α</sub></i>	1.70	1.972	1.146	0.830	0.659	(31)
<i>β<sub>α</sub></i>	86.63	63.11	48.88	39.69	33.36	-
<i>λ</i>	1	1	1	1	1	-
<i>t(m)</i>	0.0879	0.1288	0.1696	0.2105	0.2513	(13)
<i>ζ<sub>a</sub> <math>\frac{l}{t}</math></i>	2.153	1.324	0.855	0.587	0.426	(29)
<i>ζ<sub>a</sub> l (m)</i>	0.189	0.171	0.145	0.124	0,108	-
<i>ζ<sub>a</sub></i>	1.44	1.12	0.89	0.62	0.34	-
<i>l (m)</i>	0.132	0,152	0.163	0.201	0.315	-
<i><math>\frac{t}{l}</math></i>	1.0069	1.4339	1.8562	1.9098	1.4733	-
<i>Profile</i>	Nº 428	Nº 428	N_428	Nº 428	Nº 428	-
<i>Y<sub>max</sub></i>	0.00855	0.00855	0.00855	0.00855	0.00855	Table 3
<i><math>\frac{Y_{max}}{l}</math></i>	0.0649	0.056	0.0525	0.0425	0.0271	-
<i>ε</i>	0.01589	0.01537	0.01514	0.01455	0.1362	(12)
<i>ζ<sub>w</sub></i>	0.0229	0.0172	0.01348	0.00895	0.00463	(12)
<i>δ</i>	12.261	9.245	6.936	4.467	2.279	(11)
<i>β<sub>α</sub> - δ</i>	98.8944	72.3593	55.8161	44.1654	35.6455	-
<i>F<sub>r</sub> (N)</i>	5,17	5,64	6,62	7,55	8,26	(9)
<i>F<sub>s</sub> (N)</i>	325,39	367,07	437,41	518,93	606,09	(8)
<i>R</i>	1,676	1,281	1,152	1,095	1,065	(32)

In figure 3, the assemble of the propeller turbine can be seen. The main components are the runner,

the casing, the generator, shaft, guide vanes, transmit power system and the draft tube.



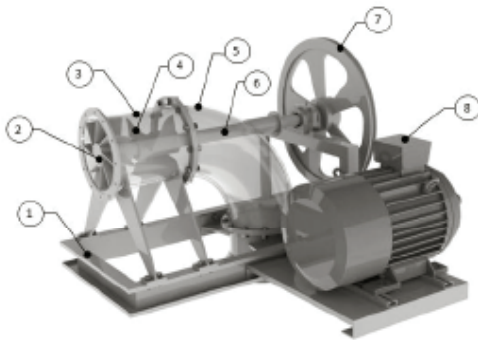


**Figure 3** Assemble of propeller turbine. 1-Support, 2-Guide vanes, 3-Casing, 4-Runner, 5-draft tube, 6-Shaft, 7-Transmit power system, 8-Generator

Using CFD modeling, the flow through the propeller turbine was analyzed and the runner design verified. These analyses were performed by means of the program Solidwork Flow Simulation that uses finite volumes theory, which shows in a graphic manner the phenomena that takes place inside the turbines. The geometrical model of the flow domain was built according to the provided specifications in the three-dimensional geometrical model of figure 3, but without the generator and the transmit power system (figure 4). As shown in figure 3, the entire fluid passageway between the inlet from the guide vanes side and the outlet from the draft tube side for the turbine is considered. The boundary conditions that were introduced at the inlet of the turbine includes the net water head ( $H$ ) and flow rate ( $Q$ ). At the outlet of the turbine, the outlet pressure was defined equal to the atmospheric pressure. Furthermore, the rotational speed of the runner wall and the shaft were also defined in the numerical model.

In figure 4, the velocity distribution inside of the propeller turbine can be seen. The flow lines show the speed of the water from the inlet, through the propeller and to the outlet. The maximum axial velocity is equal a 6.85 m/s. With the software, is also possible to determine the power output of the shaft using the torque and angular velocity of the shaft. In this case, the torque is equal to 67.99 Nm and the angular velocity is equal to 94.248 rad/s (900 rpm), thus, the power output is equal

to 6.4 kW. Figure 4 presents a correctly chosen blade profile, with correct angle of inclination for power generation.

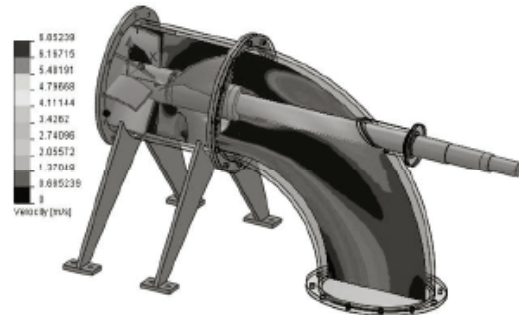


**Figure 4** Velocity distribution inside of propeller turbine

The stresses in the runner caused by the hydraulic forces also are calculated. The loads obtained from the CFD analysis for the boundary conditions are incorporated into a finite element model to calculate the stress distributions in the runner. This analysis is important to check the structural integrity of the turbine. In this study the analysis has been performed by using Cosmos Works which is an effective tool for modeling stresses. In general, the turbine blades are subjected to both, the normal and shear stresses, induced by the water flow.

A complete 3D finite element model of the runner is shown in figure 5. It consists of 3D tetrahedral elements. During the discretization process, a comparison of the convergence has been carried with respect to the mesh density. Finally, the runner is modeled with 62969 elements and 101571 nodes. Under normal operating conditions, a propeller turbine runner is subjected to two static loads, namely, the centrifugal force induced by rotation and the load due to the water pressure, and both are taken into consideration. The boundary conditions that have been used in the model are zero displacements (fixed support) at the shaft surface of runner. The material of the runner is nickel-bronze alloy due to its high strength, hardness and excellent corrosion resistance.



**Figure 5** Boundary conditions and loads for the finite element analysis

The typical stress distribution is shown in figure 6. The figure shows the major stress on the surface of the runner blade, located at the transitions between the blade and the hub. The maximum Von Mises stresses is equal to 40.3 MPa, approximately 17% of the yield strength of material; therefore, the thickness of the blades is enough to generate sufficient strength for will not break under loading.

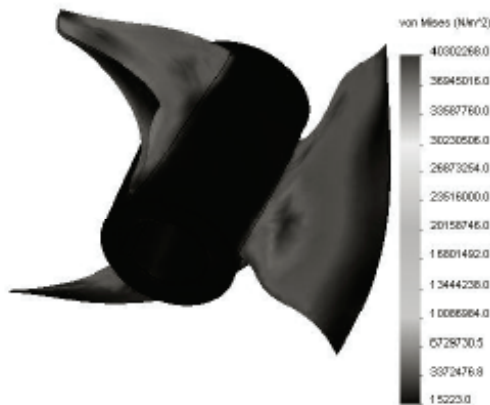


**Figure 6** Stress distribution of runner

In figure 7, displacements distribution of runner can be seen. The maximum displacement is equal to 0.00311 mm, hence the gap between the exterior diameter of runner and the casing must be greater than 0.00311 mm.

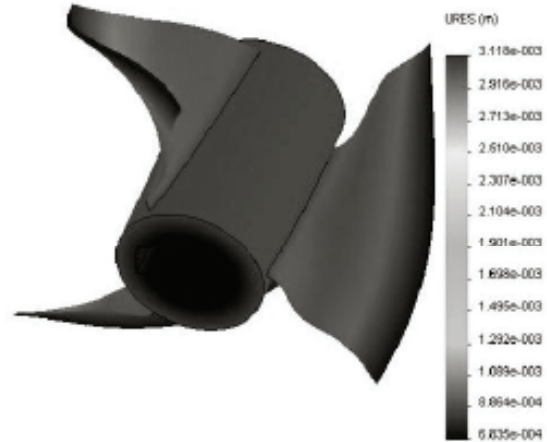


**Figure 7** Displacements distribution of runner

The first five natural frequencies and vibration shapes of the runner have also been calculated with software CAE. When the runner operates at, or close to the natural frequency, a high vibration occurs which may damage the runner, therefore, these frequencies should be different to the exciting frequency, which comes from the interaction between the runner and the stationary structure of the turbine for not cause the resonance of the hydraulic machine. Figure 8 shows one mode of vibration of the runner. This is a torsional mode. However such type of vibrations has a considerable influence on the fatigues life of the runner.

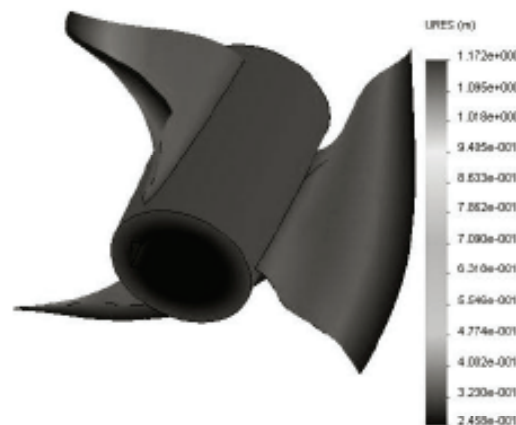


**Figure 8** Natural frequency of the runner. 5 natural modes of vibration:  $f=11.56/514.8/515.11/670.04/1716.9$  Hz.  $i=$  number of mode. Mode of vibration 1-torsional mode

Using Z Corporation 3D printing technology, the designed runner has been manufactured, and it can be dipped in wax to produce investment

casting patterns for the production. The runner prototype is shown in figure 9.



**Figure 9** Prototype of the runner

The RPT should be easily manufactured in developing countries [17]. In figure 10 the runner casing in a nickell bronze alloy can be seen.

### Conclusions

Depending on the head ( $H$ ) and discharge ( $Q$ ) of a particular site, a runner has been designed in order to get the highest efficiency. For the

preliminary hydraulic design of the runner, correlations between the geometry of runner and these parameters ( $H$ ,  $Q$ ) found in the technical literature have been used. The preliminary geometry of the runner has been checked with modern engineering tools such as Computational Fluid Dynamics (CFD) and Computer Aided Engineering software (CAE).

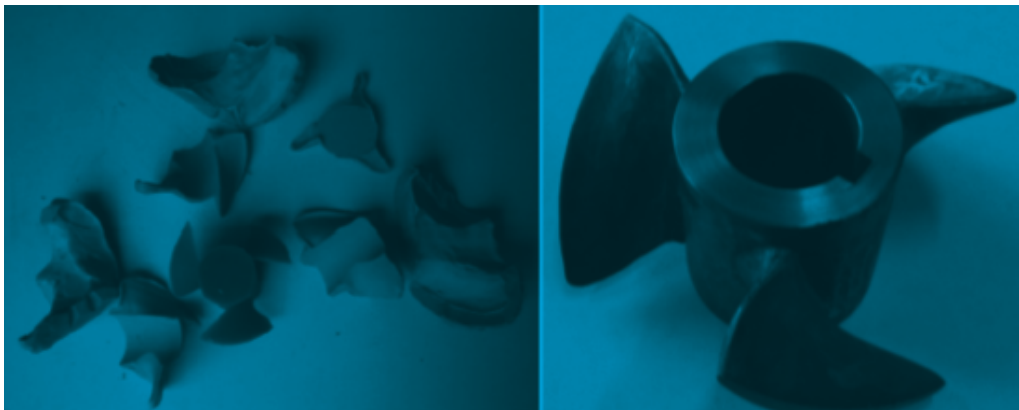


**Figure 10** Prototype of the runner casing

It has been pointed out how CFD in a graphic manner shows the phenomena which takes place inside propeller turbine. Based on the data obtained from the CFD model, a finite element analysis has been performed to identify stresses acting on the runner. It has been found that the maximum Von Mises stresses is less than the yield strength of material, therefore, the stress analysis shows that the blades are able to withstand the occurring forces inside of propeller turbine.

The runner of the propeller turbines designed can be a viable option for electricity generation in the not interconnected zones (NIZ) and can be manufactured locally.

### References

1. R. Smith, D. Vesga, A. Cadena, U. Boman, E. Larsen, I. Dyner. "Energy scenarios for Colombia: process and content". *Futures*. Vol. 37. 2005. pp. 1-17.
2. A. Williams, R. Simpson. "Pico hydro – Reducing technical risks for rural electrification". *Renewable Energy*. Vol. 34. 2009. pp. 1986-1991.
3. S. Williamson, B. Stark, J. Booker. "Low head pico hydro turbine selection using a multi-criteria analysis". *Renewable Energy*. 2012. pp. 4-11.
4. A. Brent, D. Rogers. "Renewable rural electrification: Sustainability assessment of mini-hybrid off-grid technological systems in the African context". *Renewable Energy*. Vol. 35. 2010. pp. 257-265.
5. S. Singal, R. Saini, C. Raghuvanshi. "Analysis for cost estimation of low head run-of-river small hydropower schemes". *Energy for Sustainable Development*. Vol. 14. 2010. pp. 117-126.
6. World Bank. *Technical and economic assessment of off-grid, mini-grid and grid electrification technologies-summary report*. Ed. World Bank Energy Unit. Washington, USA. 2006. pp. 155.
7. G. Demetriades. *Design of low-cost propeller turbines for standalone microhydroelectric generation units*. Doctoral Dissertation. University of Nottingham. Nottingham, United Kingdom. 1997. pp. 205.
8. D. Upadhyay. *Low head turbine development using computational fluid dynamics*. Doctoral Dissertation. UK, University of Nottingham. Nottingham, United Kingdom. 2004. pp. 195.
9. M. Kaniecki, Z. Krzemianowski. "Recent experience of IFFM PAS in the design process of low head propeller hydraulic turbines for Small Hydro". *Earth and Environmental Science*. Vol. 12 (012069). 2010. pp. 1-9.
10. G. Demetriades, A. Williams, N. Smith. "A simplified propeller turbine runner design for stand-alone microhydro power generation units". *International Journal of Ambient Energy*. Vol. 17. 1996. pp. 151-156.
11. R. Simpson, A. Williams. *Application of computational fluid dynamics to the design of pico propeller turbines*. ICRED-06, School of Engineering and Applied Sciences. University of the District of Columbia. Washington DC., USA. 2006. pp. 1-10.
12. K. Alexander, E. Giddens, A. Fuller. "Axial-flow turbines for low head microhydro systems". *Renewable Energy*. Vol. 34. 2009. pp. 35-47.
13. Y. Wu, S. Liu, H. Dou, S. Wu, T. Chen. "Numerical prediction and similarity study of pressure fluctuation in a prototype Kaplan turbine and the model turbine". *Computers & Fluids*. Vol. 56. 2012. pp. 128-142.
14. F. De Siervo, F. De Leva. "Modern trends in selecting and designing Kaplan turbines". *Water Power and Dam Construction*. Vol. 30. 1978. pp.51-57.
15. M. Adolph. *Strömungsmaschinen: Turbinen, Kreiselpumpen und Verdichter. Eine Einführung*. 1ª. ed. Ed. Springer. New York, USA. 1965. pp. 90-114.
16. C. Pfeleiderer. *Bombas centrifugas y turbocompresores*, 4ª. ed. Ed. Labor. Barcelona, España 1960. pp. 319-347.
17. E. Chica, S. Agudelo, N. Sierra. "Lost wax casting process of the runner of a propeller turbine for small hydroelectric power plants". *Renewable Energy*. Vol. 60. 2013. pp. 739-745.